

452

THE E74-LIKE FACTOR 3 (ELF3) IS A CENTRAL MEDIATOR OF CARTILAGE DEGRADATION IN A SURGICALLY-INDUCED OSTEOARTHRITIS MODEL IN MICE

E.B. Wondimu^{††}, K.L. Culley[†], J. Quinn[†], J. Chang[†], C. Dragomir[†], D. Plumb[†], M. Goldring^{††}, M. Otero-Adran[†], [†]Hosp. for Special Surgery, New York, NY, USA; ^{††}Weill Cornell Med. Coll., New York, NY, USA

Purpose: The transcription factor E74-like factor 3 (ELF3) plays a central role in mediating aberrant stress- and inflammatory signals in osteoarthritic (OA) chondrocytes. ELF3 mRNA levels are elevated in OA chondrocytes and contribute to the IL1 β -induced expression of matrix metalloproteinase 13 (Mmp13), Nos2, and Ptg2/Cox2 in vitro, indicating a pivotal role of ELF3 in cartilage degradation. Here, we aimed to investigate the contribution of gain- and loss-of-function of Elf3 to cartilage degradation in vivo.

Methods: CARTILAGE-SPECIFIC ELF3 KNOCKOUTS: We generated Col2a1Cre-driven cartilage-specific Elf3 knockout (KO) mice. We subjected 12-weeks-old male KO or control Elf3f/f (WT) littermates to the destabilization of the medial meniscus (DMM) surgical model of OA. TET-OFF INDUCIBLE ELF3-OVEREXPRESSING MICE: We generated TRE-Elf3:Comp-tTA (Tg) mice by crossing transgenic mice that express Elf3 under the control of the tetracycline-responsive element (TRE) with Comp-tTA mice expressing tTA under the control of the Cartilage Oligomeric Matrix Protein (Comp) promoter. Inducible, post-natal overexpression of Elf3 was assessed at 3, 6 and 9 months of age in Tg or Ctrl (Comp-tTA) mice. The contribution of Elf3 overexpression to spontaneously-induced OA was assessed in 6 and 9 month-old Tg and Ctrl mice. The contribution of Elf3 to the DMM-induced cartilage degradation was evaluated using 6 months-old Ctrl and Tg mice at 8-wks post-DMM surgery. SURGICAL MODEL OF OA: 12-weeks-old (WT or KO) and 6 months-old (Tg or Ctrl) male mice were subjected to the DMM surgical model of OA. DMM was performed on the right knees, while the left knees were left as unoperated controls. At 4, 8 and 12-wks (WT or KO mice) or at 8-wks (Tg and Ctrl mice) post-DMM, knees were processed for histological assessment of OA, conducted on Safranin-O/Fast green-stained serial coronal sections following OARSI guidelines. RTqPCR ANALYSIS: Total RNA was isolated from the articular cartilage of control and DMM-operated WT and KO mice at 8-wks post-DMM. The total RNA was reverse-transcribed and amplified using SYBR Green I-based qPCR and specific primers for Elf3, Mmp13, Nos2, and Ptg2. Data were normalized using Eef1a1, Gapdh and Hprt1 as housekeeping genes.

Results: Histological assessment of OA severity showed attenuation of cartilage loss at 8 and 12 wks post-DMM surgery in KO mice compared to WT animals. We observed reduced MMP13-mediated collagenase activity, and decreased expression of Mmp13, Nos2, and Ptg2/Cox2, assessed by RTqPCR analysis, in KO mice at 8-wks post-DMM. Importantly, while the TRE-Elf3:Comp-tTA (Tg) mice showed a trend towards increased cartilage damage at 6 and 9 months of age, the DMM-operated Tg mice exhibit significantly increased cartilage loss compared to Ctrl counterparts, suggesting that biomechanical challenge may be required to fully activate Elf3.

Conclusions: Here, we provide evidence that Elf3 is a central contributing factor for cartilage degradation in vivo, in OA disease. Cartilage-specific Elf3 deficiency protects against surgically-induced OA and Elf3 overexpression results in exacerbated cartilage degradation in mice subjected to the DMM surgery. Cartilage-specific Elf3 knockout mice have decreased MMP13/collagenase activity and decreased expression of several Elf3 target genes, including Mmp13. Our results are consistent with previous reports in vitro; showing reduced IL-1 β -driven Mmp13 expression in murine Elf3^{-/-} chondrocytes and in human OA primary chondrocytes with siRNA-mediated ELF3 knockdown. Together, our in vivo and in vitro data represent strong evidence of a central role of Elf3 in the pathogenesis of OA, by controlling Mmp13-mediated collagen degradation. Thus, a better understanding of the mechanisms of action of Elf3 in chondrocytes will lead to the identification and development of targeted therapies for OA.

453

ACUTE MITOCHONDRIAL DYSFUNCTION IN CARTILAGE FOLLOWING MECHANICAL INJURY

M.L. Delco, Cornell Univ., Ithaca, NY, USA

Purpose: Mitochondria (MT) mediate the pathogenesis of many complex and unrelated diseases. MT dysfunction occurs secondary to mechanical injury in syndromes such as fluid shear-induced atherosclerosis and intraocular pressure-induced retinopathy in glaucoma. Trauma to cartilage can initiate post-traumatic osteoarthritis (PTOA) however the mechanisms are not fully understood. Evidence supports MT dysfunction in established OA, however the role of MT dysfunction in the early pathogenesis of PTOA is not clear. The goal of this study was to evaluate MT dysfunction the peracute (within hours) response of cartilage to traumatic injury, and to determine the relationship between MT function and early PTOA. A novel adaptation of the technique of real-time microscale respirometry to evaluate early post-traumatic chondrocyte MT function in situ is described.

Methods: Cartilage was harvested from knees of neonatal bovines. Explants were subjected to unconfined compression (4-8 MPa peak stress; 5-10 GPa/s peak stress rate) using a validated sub-critical damage model. Explants were then divided for use in 3 assays (Fig 1); MT function was assessed in real time by microscale respirometry, MT membrane potential was measured by polarity-sensitive fluorescent staining, and chondrocyte viability was evaluated on confocal microscopy. Microscale respirometry was performed on explants loaded into a 24-well tissue capture microplate and analyzed in a Seahorse XF 24 analyzer. Glycolysis and oxidative phosphorylation were quantified every 8 minutes for a total of 245 minutes by measuring extracellular acidification (ECAR) and oxygen consumption rates (OCR), respectively. To measure specific indices of MT function, a MT stress test was performed by sequentially adding 1) oligomycin, an ATP synthase inhibitor 2) FCCP, a proton circuit uncoupler 3) rotenone + antimycin A (inhibitors of MT complexes I and III) to determine ATP turnover, spare respiratory capacity and proton leak across the inner MT membrane, respectively. Relative MT membrane potential was measured by the fluorescent intensity ratio of a polarity-insensitive MT fluorescent probe (MitoTracker Green) to a polarity sensitive MT marker (TMRM) on confocal microscopy.

Results: Baseline OCRs were higher in control samples than impacted samples and higher in cartilage from the femoral condyle than the patellofemoral groove (Fig 2). Within two hour of injury, explants displayed impaired respiratory control in response to respiratory inhibitors (Fig 2). Most notably, injured samples demonstrated an attenuated response to FCCP with a 61% (range 43-71) decrease in spare respiratory capacity. Significant differences in ECAR between groups were not detected. Cell viability was decreased in impacted samples by an average of 20% (range 5-38) versus non-impacted controls (Fig 2A). MT membrane potential was decreased in impacted samples versus control (Fig 3), indicated by a 34% (range 3-54) decrease in red:green (polarized MT:all MT) fluorescent intensity ratio after injury.

Conclusions: This study revealed that MT dysfunction is a peracute response of chondrocytes to mechanical injury. Over the described range of impact magnitudes, cartilage compression resulted in decreased basal respiration, compromised ATP turnover and reduced maximal respiratory capacity, indicating likely inhibition of electron transport in the mitochondrial respiratory chain. This is the first report of adapting microscale respirometry to study the subcellular mechanisms of impact-induced MT dysfunction. This model allows real time

monitoring of chondrocyte MT function in whole cartilage, and offers the opportunity to test drugs to prevent/reverse MT dysfunction after cartilage trauma.

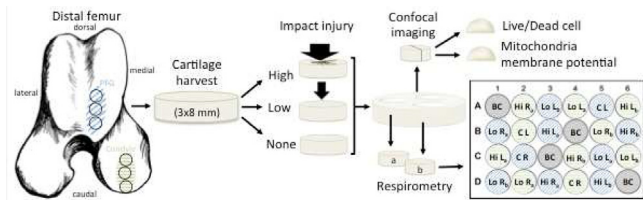


Fig. 1. **Experimental design.** For the example microrespirometry plate layout, Hi = high impact, Lo = low impact, C = no impact, L = left limb R = right limb, BC = background $[O_2]$ correction wells.

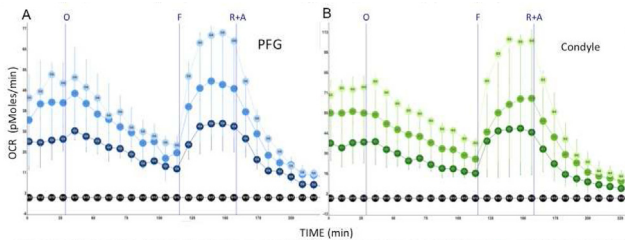


Fig. 2. **Respirometry in injured cartilage.** Data represents OCR over time. A) Impacted cartilage from the PFG (○ = low impact, ● = high impact) display lower basal OCRs (0–30 min) than controls (●) and an altered response after addition of oligomycin (O), FCCP (F), and rotenone/antimycin A (R+A). B) The same trends occur in the condyle (B) but basal OCRs are higher. ● = control, ○ = low impact, ● = high impact. ● = background $[O_2]$ correction data.

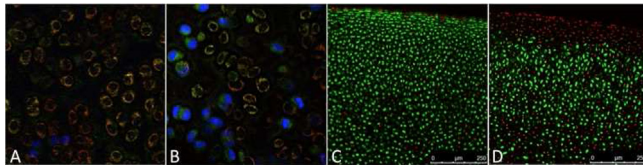


Fig. 3. **Cartilage injury results in MT depolarization and cell death.** Confocal images of (A) control and (B) impacted cartilage stained with MitoTracker Green (green; all MT), TMRM (red; polarized MT only) and Hoechst 33342 (blue; nuclei). Green-only stained MT with increased uptake of nuclear stain indicates compromised integrity of both the cell and MT membranes. Calcein AM/ethidium homodimer (green/red; live/dead cell) staining of control (C) and impacted (D) explants.

454

MAGNETIC RESONANCE IMAGING SEMI-QUANTITATIVE SCORING SYSTEM OF SYNOVITIS AFTER ANTERIOR CRUCIATE LIGAMENT TEARS

K. Amano[†], M. Kretschmar[†], M. Lee^{††}, C. Ma[†], X. Li[†], T. Link[†]. [†]Univ. of California, San Francisco, San Francisco, CA, USA; ^{††}Asan Med. Ctr., Univ. of Ulsan Coll. of Med., Seoul, Republic of Korea

Purpose: Anterior cruciate ligament (ACL) injuries can lead to development of early osteoarthritis (OA) in the young and active, specifically post-traumatic osteoarthritis (PTOA), despite surgical reconstruction. While multiple biomechanical and molecular factors may contribute to the development of PTOA, inflammation has garnered attention as a possible contributor to the onset of joint degeneration. The current standard imaging method to diagnose synovitis is contrast enhanced fat suppressed MRI imaging. In this study, we propose a new semi-quantitative scoring system for synovitis that utilizes non-contrast MRI sequences. The purpose of this study was to assess the feasibility of this new scoring system and to note its characteristic findings on ACL injured knees.

Methods: Bilateral knees of 48 patients (27 males; age $32.5 \pm SD 8.4$ years) with acute isolated ACL tears were scanned using a 3 Tesla MRI scanner (GE Healthcare) with an 8-channel phased array knee coil (Invivo) prior to surgical reconstruction. Patients were recruited within six months of their injury ($52 \pm SD 25$ days after injury). Imaging protocols included (1) high-resolution 3D FSE (CUBE), TR/TE = 1500/26.69

ms, field of view 16 cm, 384 x 384 matrix size, slice thickness 0.5 mm, echo train length 32; and (2) sagittal T2 FSE with TR/TE = 4000/(30–60) ms, slice thickness of 1.5 mm, spacing of 1.5 mm, field of view 16 cm, 512 x 512 matrix size and echo train length 9. For the T2 FSE sequence, the patients were scanned in the extended and flexed ($\sim 30^\circ$) positions with 25% body weight applied axially. The images were analyzed by 3 musculoskeletal radiologists, and Whole Organ Magnetic Resonance Imaging Scores (WORMS) were recorded for each knee MRI. For the new synovitis scoring system, four radiological parameters of synovitis were used: Hoffa Synovitis (HS), Joint Effusion (JE), Synovial Thickening (ST), and Synovial Proliferation (SP). HS was assessed with hyperintensity seen in Hoffa's fat pad in the sagittal CUBE sequence. JE was scored by measuring the thickness of fluid accumulation in the suprapatellar recess on the mid-sagittal CUBE sequence. ST was scored by the thickness of the synovial membrane at the suprapatellar recess in the T2 FSE sequence. SP was assessed by evaluating synovial bands and irregularities seen in the suprapatellar synovial membrane in the CUBE and the T2 FSE sequences (Table 1 and Image 1). Inter-rater agreement was measured by Cohen's kappa between two musculoskeletal radiologists. Multivariate linear regression was used to assess the association of the synovitis score with the WORMS, with age BMI, and days from injury as covariates. To investigate differences between low and high synovitis scores with respect to the WORMS grades, adjusted least square means of the outcome measures were tested with Student's t-test.

Results: Cohen's kappa scores were 0.819, 0.946, 0.833, 0.846 for HS, JE, ST, and SP respectively in 29 scans, randomly selected from the original 48 for reliability. Table 2 shows the prevalence of each scoring. Days from injury correlated negatively with JE ($p=0.0402$). There were significant difference in the WORMS ligament score between high and low SP scores ($p=0.0454$), and in the WORMS effusion score between high and low HS scores (0.0043), with positive correlation. No correlations were found between synovitis grades and the total WORMS, different grades of cartilage, bone marrow, and menisci.

Conclusions: The new synovitis scoring system using non-contrast MRI sequence, which showed good inter-rater reliability across all four parameters, is a promising system for quantifying the extent of synovitis in a knee joint. A high prevalence of synovitis related findings was found in this cohort of patients with subacute ACL tears in this scoring and WORMS. However, a negative correlation between the Joint Effusion component and days from injury indicates a decline of the inflammatory response with time. In this subacute phase, the synovitis measured is more likely related to a reparative response. Whether these early findings are related to possible chronic inflammation with long term follow up and contribute to joint degeneration on the long run has to be investigated with a longitudinal study with comparisons with normal knees.

Funding: NIH/NIAMS P50 AR060752 grant.

